Variation of Critical Rainfall Duration upon Its Magnitude in Middle and Lower Yom Basin, Thailand

P. Klongvessa*[1], M. Lu[2], S. Chotpantarat[3]

[1,2]Department of Civil and Environmental Engineering, Graduate School of Engineering, Nagaoka university of Technology, Kamitomioka 1603-1, Nagaoka, Niigata 940-2188, Japan

[3]Department of Geology, Faculty of Science, Chulalongkorn University, 254 Phyathai Road, Pathumwan, Bangkok 10330, Thailand

[3]Research Program in Control of Hazardous Contaminants in Raw Water Resources for Water Scarcity Resilience, Center of Excellence on Hazardous Substance Management (HSM), Chulalongkorn University, 254 Phyathai Road, Pathumwan, Bangkok 10330, Thailand

*[1]nineboon@hotmail.com; [2]lu@nagaokaut.ac.jp; [3]csrilert@gmail.com

Abstract-**In many flood simulations, critical rainfall duration, defined as duration of rainfall which causes a critical flood, is assumed to be fixed. However, in some area, the critical rainfall duration varies upon its magnitude and assuming the fixed critical rainfall duration may underestimate an extreme peak discharge. The middle and lower Yom basin, Thailand, is one of the areas where a larger flood appears to coincide with longer critical rainfall duration. In this study, we have investigated the variation of critical rainfall duration in that area. The conceptual model was developed from HEC-HMS and HEC-RAS models. The upstream and downstream parts of the area were calibrated separately. Then, uniform 2-, 5-, and 10-year rainfalls with 24-, 48-, and 72-hour durations were simulated. The model successfully reproduced the variation of critical rainfall duration as 48 hours for 2- and 5-year rainfalls and 72 hours for 10-year rainfall. This variation is caused by a high percolation rate over the upstream area. With this percolation, some portion of rainfall over the upstream part is loss. Hence, most of the flood water comes from the downstream part which has short travel time. However, when the rainfall is larger, the influence of percolation is less.**

Keywords- Critical Rainfall Duration; Flood; Yom Basin; Percolation

I. INTRODUCTION

In extreme flood simulations, the duration of the simulated rainfall is usually equal to the travel time of the water from the most remote part of the basin to the outlet, known as concentration time, because it generally leads to the critical flood [1]. In other words, the concentration time is usually used as the critical rainfall duration, the duration of rainfall which causes the critical flood. Since the concentration time is related with the delay time between rainfall and peak discharge, known as lag time, whether the critical rainfall duration is constant depends on whether the lag time is constant. Conceptually, the lag time can be calculated as the volume-weighted average travel time of water from each part of the basin to the outlet [2]. However, due to the complexity to handle the spatial data, many of the simulations assume the uniform rainfall and basin characteristics. These assumptions cause the lag time to be constant. Therefore, the critical rainfall duration is implicitly assumed to be constant. Nevertheless, in large areas such as Yom basin, Thailand, most of the flood simulations may take the rainfall spatial distribution into account. One of the interesting simulations was done by Tingsanchali and Karim [3]. This study interestingly established the flood maps from 20-, 50-, 100-, and 200-year rainfalls. However, the simulated rainfalls were still under the same duration for all rainfall magnitudes. In other words, the critical rainfall duration was still assumed to be constant.

In reality, the critical rainfall duration may not be constant. For example, in Thailand, the Royal Irrigation Department (RID) has developed the plan for flood mitigation which includes the estimation of river water level at the downstream station from the water level at the upstream station [4]. This plan also mentions the delay time of the estimated downstream water level after the observed upstream water level. The data concluded in that plan reveals that depending on the area, the delay time may be constant, shorter for larger flood, or shorter for smaller flood. This finding probably infers that the lag time between rainfall and peak flood can vary upon the rainfall magnitude. For Yom basin, the area where the variation of the delay time is very obvious, the delay time is shorter for the smaller flood and longer for the larger flood in the middle and lower parts, while it is opposite for the upper part. Therefore, in the middle and lower parts of the Yom basin, the larger rainfall may have longer critical duration. In flood mitigation, ignoring the variation of critical rainfall duration may cause the underestimation of the extreme peak discharge under some specified return period.

In this study, we identified the variation of critical rainfall duration as well as physical mechanism behind this variation in the middle and lower parts of the Yom basin. The area is shown in Fig. 1. The special feature of this area is that there is no large scale control structure to control the river flow except the Mae Yom weir at the upstream point and small floodgates along the river for the irrigation purpose. Therefore, the water flows naturally from the upstream mountainous region to the

DOI:10.5963/JWRHE0603001

downstream plain area. We have developed the model which can reproduce the variation of critical rainfall duration in the area and investigated how this variation is produced in the model.

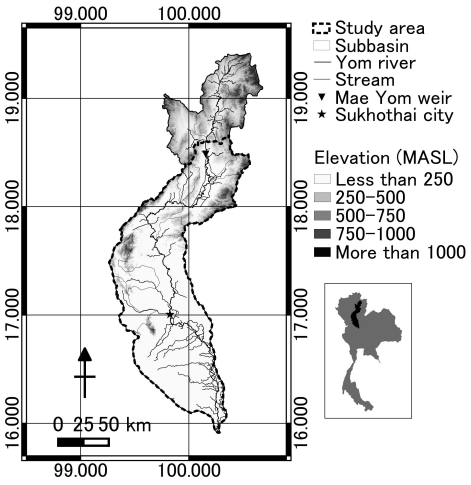

Fig. 1 Study area

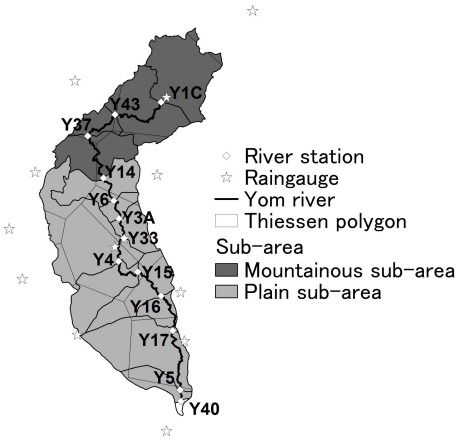

Fig. 2 Modelling sub-areas, river, river stations, and raingauges

II. METHODOLOGY

A. Model Development

1) Model Digitization:

In this study, HEC-HMS model was applied to simulate a runoff from rainfall and HEC-RAS model was applied to simulate a flow in Yom River in the middle and lower Yom basin. There are 13 stations along the river where flows and water levels have been observed by RID. Locations of these stations are shown in Fig. 2. At the stations Y1C, Y43, and Y37, the flows and water levels have been collected hourly, while they have been collected 5 times a day at the others station. For the rainfall data, it has been collected every 3 hours by Thai Meteorological Department (TMD) at 13 stations over and nearby the area. Locations of these stations are shown in Fig. 2. Daily pan evaporation data has also been collected at these TMD stations. The cross-sections used in the model were as of the surveys by RID between the end of the year 2013 and the beginning of the year 2014 which were done at the same points that the water levels and flows have been observed.

In HEC-RAS model, the discharge at the station Y1C was used as an upstream boundary condition and the water level at the station Y40 was used as a downstream boundary condition as shown in Fig. 2. The distance along the river from the station Y1C to the station Y40 is approximately 500 km. Lateral flows from river branches were included as uniform lateral flows between the stations Y1C and Y6 and between the stations Y33 and Y4 since these locations have lots of river branches which contribute large amounts of lateral flows. Also, there is a diversion canal between the stations Y6 and Y3A which was included in the model as a lateral diversion structure. In the simulation, the flow in the river was calculated by the principles of conservation of mass and conservation of momentum [5] with the timestep of 15 minutes and distance between computation points of not more than 5 km. The runoff from rainfall was included in the model as a lateral flow to each of the 13 river stations which was calculated by HEC-HMS model.

DOI:10.5963/JWRHE0603001

In HEC-HMS model, the study area was divided into 13 sub-areas as shown in Fig. 2. The total size of these 13 sub-areas was approximately 19,000 km^2. Each area contributed runoff to each of the 13 river stations. Usually, the topography was used to define the boundaries of the sub-areas. However, some parts of the area were too flat to define the boundaries. In that case, the assumption that the runoff was drained to the nearest stream was applied to divide the area. After the area had been divided, the rainfall and evaporation for each sub-area were calculated by Thiessen-weighted average of the TMD data. The rainfall data was input every 3 hours while the evaporation data was input as the monthly average. In the simulation, runoff from the rainfall was calculated by deficit and constant infiltration, Snyder unit hydrograph transformation, and recession baseflow with the timestep of 15 minutes. Details of these calculation schemes can be seen in the technical reference of HEC-HMS model [6].

2) Model Calibration and Verification:

There were 8 model parameters to calibrate, Manning's n of the channel (n), surface storage capacity (max $S_{surface}$), standard lag (t_p) and peaking coefficient (C_p) for the Snyder unit hydrograph transformation, ratio to peak (Q_0/Q_p where Q_0 was discharge amount at which baseflow began and Q_p was the peak discharge before an occurrence of the baseflow) and recession constant (k) for the baseflow model, and infiltration storage capacity (max $S_{infiltration}$) and constant rate or percolation rate (f_c) for the loss model. Details of these parameters can be seen in the technical references of HEC-RAS and HEC-HMS models [5-6]. Out of these 8 parameters, most of them were calibrated directly. The exception was only the standard lag for the Snyder unit hydrograph transformation (t_p) which was obtained from a calibrated basin coefficient (C_t) and calculated by Equation (1) [6]:

$$t_p = 0.75 C_t (L L_c)^{0.3} \tag{1}$$

where L was a stream length from an outlet to a boundary in kilometers, L_c was a stream length from an outlet to the point closet to the centroid of the area in kilometers, and t_p was the standard lag in hours.

In this study, data during the wet season in 2013 and 2014 were used for the calibration. The simulated water levels were compared with the observed ones at the stations Y37, Y14, Y6, Y3A, Y33, and Y4. The comparison was not done at the others station because the data was not of a very good quality at the station Y43 and the water level was influenced by flow over the flood plain due to the small river size and the flatness of the area at the stations Y15, Y16, Y17, and Y5. Moreover, the flood mitigation plan [4] clearly mentions the estimation of water level only from the upstream to the station Y4, which is in the urban area named Sukhothai city. Therefore, the station Y4 was the station we paid attention for. The simulation was done from April to October of each year, but April was considered as a spin-up period to eliminate the influence of initial conditions. Therefore, the calibration was done only from May to October. After the calibration, the model was verified with observed data from May to October in 2011 and 2012. The data before 2011 was not used since the year 2011 was the year of big flood which caused large changes in cross-sections.

The important characteristic of the study area which was suspected to cause the variation of critical rainfall duration is a difference of characteristics between the upstream mountainous region and downstream plain area. The downstream plain area is characterized by clay as a major soil texture, agricultural area as a major land cover, and flat topography. The upstream mountainous region is composed of coarser soil, has forest area as a major land cover, and has more steepness. Hence, the mountainous region was calibrated separately from the plain area. In this study, we used the station Y14 as the boundary between these 2 parts (see Fig. 2).

3) Model Simplification:

After the verification, the model was proved to simulate the water level accurately. However, with 13 sub-areas, there was a need to process 13 sets of data. It would be easier if the sets of data to process were less. Hence, before the experimental simulation, we tried to reduce the need to process 13 sets of data.

The study of Lee et al. [7] has suggested that if the area is not very large, rainfall spatial distribution does not affect the basin discharge. Hence, if the area is small enough, assuming the uniform rainfall is acceptable. As a result, we could use the same rainfall data for some sub-areas if they are closed to one another and total area is not very large. Accordingly, we grouped some sub-areas together and used the same rainfall hyetograph within each group. The rainfall amount we used was the average rainfall among sub-areas in the group.

We grouped the sub-areas as much as possible to make the model simplest. However, if the group size was too large, the simulated water level could be inaccurate. Therefore, the accuracy of the simulated water level should be checked while trying to use the average rainfall among the group of sub-areas. If it was not accurate, the average rainfall could not be used for the entire group, and therefore, the group should be split. Since the evaporation data has been collected at the same location where the rainfall data has been collected, the evaporation was averaged in the same way.

B. Experimental Simulation

In the experimental simulation, the rainfall was designed and input to the developed model to determine a peak discharge. Since we aimed to simulate the variation of critical rainfall duration due to its magnitude, we variated both rainfall duration

DOI:10.5963/JWRHE0603001

and magnitude. The rainfall magnitudes simulated in this study were the magnitudes of 2-, 5-, and 10-year rainfalls as of the result of frequency analysis using generalized extreme-value (GEV) distribution the detail of which is discussed in section II-B-1. The simulated rainfall was spatially uniform. In other words, rainfall magnitudes over the all parts of the area were equal. The simulated rainfall durations were 24, 48, and 72 hours. The rainfall temporal distribution was determined by alternating block method the detail of which is discussed in section II-B-2. In the model, initial soil moisture was set to be saturated because the heavy rainfall during the mid-rainy season usually causes the soil to be mostly saturated in flood years [8]. Therefore, in our model, the loss for the rainfall was determined by the constant percolation rate (f_c).

1) Frequency Analysis:

The magnitude of simulated rainfall was determined by frequency analysis. The data used for the frequency analysis was the area-weighted average rainfall determined by Thiessen polygons. For each year during 1981-2010, the observed maximum 24-, 48-, and 72-hour rainfalls between May and October were selected. For each of these durations, the Weibull equation [9] was applied to calculate the occurrence probabilities of that observed maximum rainfall magnitudes. Then, GEV distribution was used to fit the data with the least squares method. In GEV distribution, magnitude of maximum rainfall (x) was described as Equation (2) [10]:

$$x = \begin{cases} \xi + \dfrac{\alpha}{\kappa}[1-(-\ln(1-p))^{\kappa}] & ;\kappa \neq 0 \\ \xi - \alpha \ln(-\ln(1-p)) & ;\kappa = 0 \end{cases} \tag{2}$$

where p was an exceedance probability, ξ was a location parameter, α was a scale parameter, and κ was a shape parameter.

2) Hyetograph Design:

The data used for hyetograph design were hyetographs of the observed rainfalls within each part of the area which contain the period of 24 hours with more than 35.0 mm rainfall depth. The criterion of 35.0 mm was used because it is the same criterion that TMD uses to classify the day as heavy rainfall day.

Within each part, all heavy rainfall hyetographs were converted dimensionless in both time and magnitude. Then, alternating block method was applied. In the alternating block method, the highest intensity in each hyetograph was put to the middle of the period. Then, the second-highest intensity was put to the right of the highest intensity and the third-highest intensity was put to the left of the highest intensity. Next, the fourth-highest intensity was put to the right of the second-highest intensity and the fifth-highest intensity was put to the left of the third-highest intensity. For the remaining lower intensities, the similar process was done until the lowest intensity was reached. By this method, all dimensionless rainfall hyetographs were converted to have high intensity in the middle and low intensity in the tail. After that, these dimensionless hyetographs from all selected events were averaged.

The average dimensionless hyetograph was converted to the designed hyetograph with the specific magnitude and duration by multiplying the dimensionless magnitude by the actual magnitude and multiplying the dimensionless time by the actual duration.

III. RESULTS AND DISCUSSION

A. Developed Model

1) Parameters:

The results of the calibration are shown in Table 1. In comparison between the mountainous region and plain area, the plain area has higher value of C_t while the mountainous region has higher values of n and f_c. The higher value of C_t over the plain area coincides with the flat topography. The higher values of n and f_c over the mountainous region coincide with coarser soil texture and higher infiltration capacity due to the forest area, respectively. Therefore, this model successfully represents the difference of characteristics between the mountainous region and plain area.

TABLE 1 CALIBRATED PARAMETERS

Parameter	Mountainous region	Plain area
n	0.047	0.019
max $S_{surface}$	0 mm	30 mm
C_t	2.9	5.8
C_p	0.16	0.18
Q_0/Q_p	0.25	0.20
k	0.87	0.89
max $S_{infiltration}$	285 mm	320 mm
f_c	2.95 mm/h	0.45 mm/h

DOI:10.5963/JWRHE0603001

2) Model Accuracy:

The model can simulate the water level accurately for the years 2012, 2013, and 2014. For the year 2011, the root-mean-square error (RMSE) appears to be larger because of the changes in cross-sections due to the big flood in 2011. In comparison between the mountainous region and plain area, the RMSE in the plain area seems to be worse because of a water diversion for irrigation between Yom basin and the nearby basin, Nan basin, at the stations Y3A, Y33, and Y4. The RMSE at all stations are shown in Table 2. The observed and modelled water levels at the station Y4, which represents the flood in the Sukhothai city, and station Y14, which represents the discharge from the mountainous region, are shown in Fig. 3. At the station Y14, the water level is not influenced by the flow in the downstream area.

TABLE 2 RMSE OF SIMULATED WATER LEVEL

Station	RMSE (m)			
	Year 2011	Year 2012	Year 2013	Year 2014
Y37	0.83	0.55	0.33	0.30
Y14	1.04	0.79	0.66	0.59
Y6	0.99	0.82	0.70	0.78
Y3A	1.48	1.02	0.80	0.58
Y33	1.51	1.01	0.60	0.62
Y4	0.90	0.82	0.89	0.74

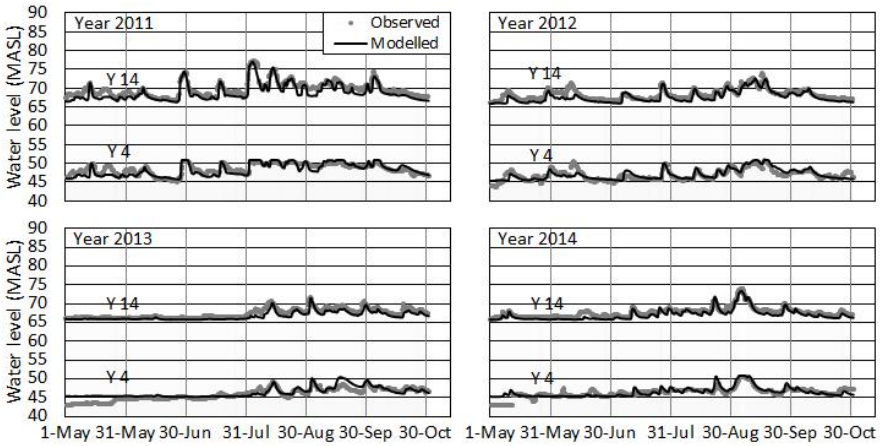

Fig. 3 Observed and modelled water levels at the stations Y14 and Y4

3) Simplified Model:

As mentioned in the section II-A-3, we reduced the need to process 13 datasets for 13 sub-areas by grouping some sub-areas together and averaging the rainfall amount within each group. After the numerous ways of grouping were carried out, we have found that the sub-areas can be grouped into 4 zones and there is no need to simulate rainfalls over the sub-areas Y15, Y16, Y17, Y5, and Y40 because the water levels at these stations do not affect the water level at the station Y4, which represents the flood in the Sukhothai city. The 4 zones from the result of sub-area grouping will be referred as zone 1, zone 2, zone 3, and zone 4. The zone 1 is the most upstream part and the zone 4 is the most downstream part. The boundaries of these zones are shown in Fig. 4. The simulated water levels from the cases before the simplification (control case), after the simplification (optimum case), and when all sub-areas are grouped into 1 zone (lumped case), at the stations Y14 and Y4 are shown in Fig. 5. The maximum difference between peak water levels simulated from the control and optimum cases as well as that between peak water levels simulated from the control and lumped cases is shown in Table 3. The result for the lumped case in the year 2011 is not shown in Fig. 5 and Table 3 because the water level goes below the river bed in some period.

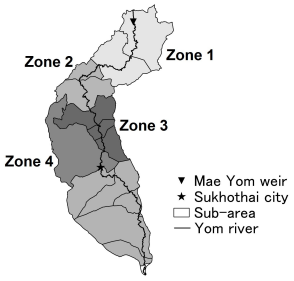

Fig. 4 Zones where the same rainfall data is used

DOI:10.5963/JWRHE0603001

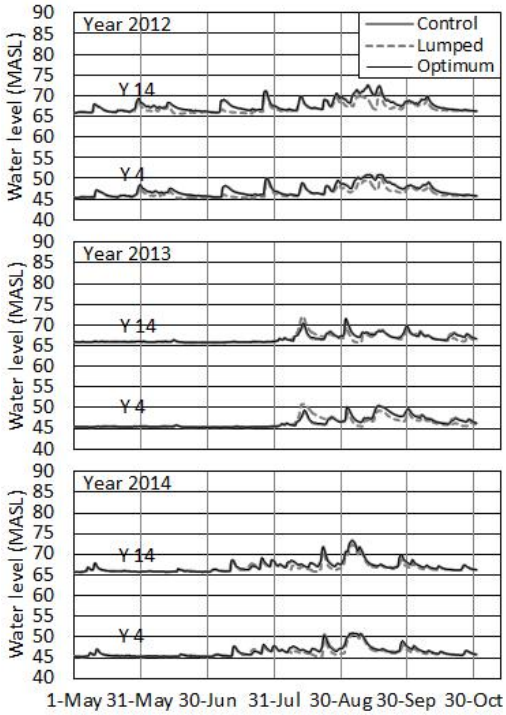

Fig. 5 Simulated water levels from control, optimum, and lumped cases at the stations Y14 and Y4

TABLE 3 MAXIMUM DIFFERENCES BETWEEN SIMULATED PEAK WATER LEVELS FROM THE CONTROL AND OPTIMUM CASES (OUTSIDE THE PARENTHESIS), AND THOSE BETWEEN SIMULATED PEAK WATER LEVELS FROM THE CONTROL AND LUMPED CASES (INSIDE THE PARENTHESIS)

Station	Difference between water levels (m)			
	Year 2011	Year 2012	Year 2013	Year 2014
Y37	0.59 (-)	0.21 (2.88)	0.33 (1.75)	0.33 (1.16)
Y14	0.64 (-)	0.25 (2.59)	0.31 (1.97)	0.27 (1.14)
Y6	0.58 (-)	0.17 (2.34)	0.29 (2.10)	0.25 (1.22)
Y3A	0.64 (-)	0.27 (2.98)	0.35 (2.62)	0.30 (1.43)
Y33	0.70 (-)	0.28 (3.04)	0.33 (2.48)	0.28 (1.35)
Y4	0.54 (-)	0.22 (2.10)	0.27 (1.69)	0.23 (1.15)

In comparison between the lumped and control cases, the differences of simulated peaks can be in terms of a few meters. These differences are even more than the model errors (see RMSE in Table 2). On the other hands, in comparison between the control and optimum cases, the differences between simulated water levels are as small as a few ten centimeters and are mostly less than the model errors. Therefore, it is not appropriate to group all of the 13 sub-areas into 1 zone, but it is adequate to group the sub-areas into 4 zones.

B. Design Rainfall

1) Rainfall Magnitude:

The GEV probability distribution appears to estimate the extreme rainfall magnitude accurately with the RMSE of approximately 4 mm. The magnitudes are remarkably high in the years with high extreme rainfall magnitudes but not far different from the average in the years with low extreme rainfall magnitudes. The parameters of the GEV probability distributions of the extreme 24-, 48-, and 72-hour rainfalls in the area as well as the RMSE between observed and expected rainfall magnitudes are shown in Table 4, the observed and expected rainfall magnitudes are shown in Fig. 6, and the magnitudes of 2-, 5-, and 10-year rainfalls are shown in Table 5.

TABLE 4 PARAMETERS USED IN GEV DISTRIBUTION FOR FREQUENCY ANALYSIS OF 24-, 48-, AND 72-HOUR RAINFALLS AND RMSE

Duration (hour)	Parameter			RMSE (mm)
	ξ	α	κ	
24	51.81070	14.38137	-0.33115	4.4
48	72.09355	14.66358	-0.53568	4.0
72	86.09529	16.19387	-0.52572	3.8

DOI:10.5963/JWRHE0603001

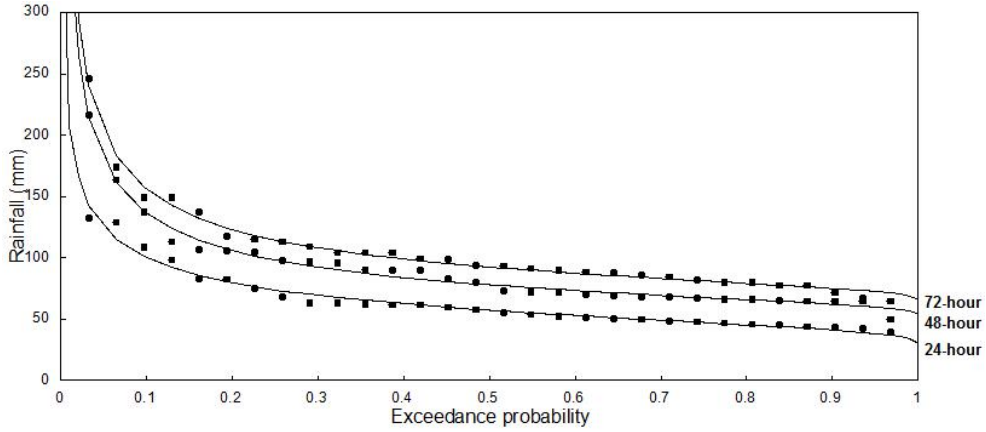

Fig. 6 Observed and expected magnitudes of extreme rainfalls

TABLE 5 MAGNITUDES OF 2-, 5-, AND 10-YEAR RAINFALLS

Duration (hour)	Rainfall magnitude (mm)		
	2-year	5-year	10-year
24	57.4	79.7	99.9
48	78.0	105.9	136.1
72	92.6	123.1	155.8

2) Rainfall Hyetograph:

The dimensionless cumulative mass curves of the hyetographs developed by the alternating block method are shown in Fig. 7. Their positions are between 10-th and 90-th percentiles of the dimensionless cumulative mass curves of the observed rainfalls. Therefore, these developed dimensionless hyetographs can represent the rainfall in the area.

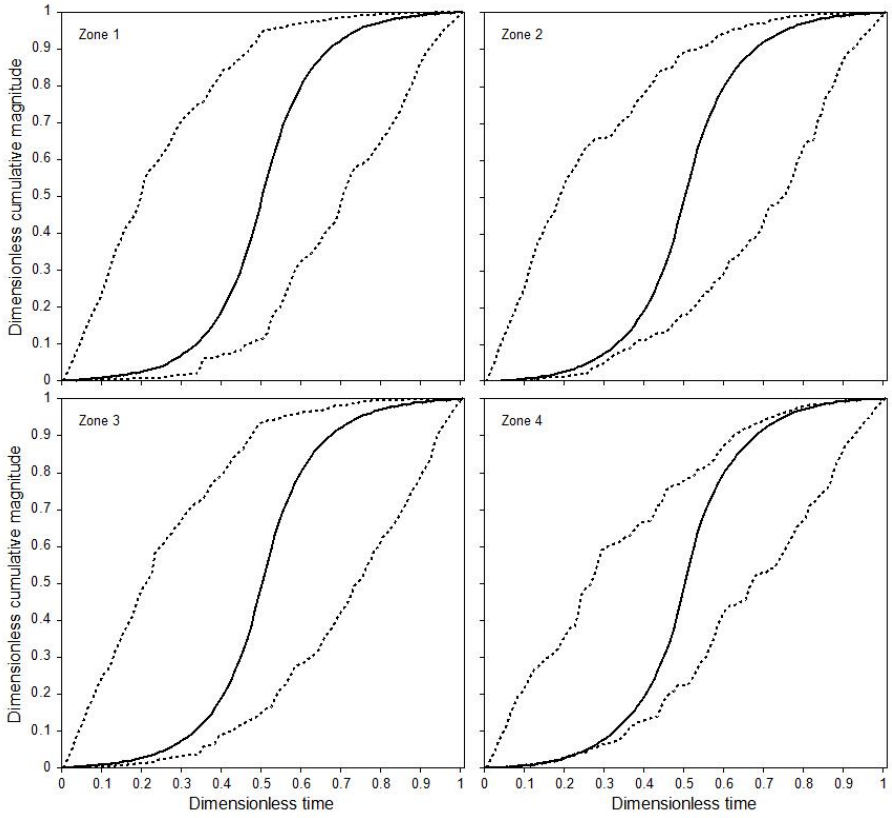

Fig. 7 Dimensionless cumulative mass curves of design rainfalls (continuous line) and those of 10-th percentile (lower dotted line) and 90-th percentile (upper dotted line) of observed rainfalls

DOI:10.5963/JWRHE0603001

C. Simulated Discharge

The peak discharges from 2-, 5-, and 10-year rainfalls with the durations of 24-, 48-, and 72-hour are shown in Table 6. It can be seen that the critical rainfall duration is longer when the rainfall is larger. For 2- and 5-year rainfalls, the maximum floods occur with 48-hour rainfall duration while for 10-year rainfall, the maximum flood occurs with 72-hour rainfall duration. Therefore, our model successfully simulates the variation of critical rainfall duration.

TABLE 6 PEAK DISCHARGES FROM 2-, 5-, AND 10-YEAR RAINFALLS UNDER DIFFERENT DURATIONS

Duration (hour)	Peak discharge (m^3/s)		
	2-year	5-year	10-year
24	415.6	792.8	1186.7
48	455.1	910.6	1457.5
72	433.5	895.9	1461.9

The physical mechanism behind the variation of critical rainfall duration can be described by the excess rainfall intensity, which is the intensity of the remaining part of rainfall after the losses due to percolation and surface storage. Even though the simulation of uniform rainfall causes all of zones 1-4 to have same rainfall amount, the different of percolation rates among these zones causes the excess rainfall amounts to be different. Zones 1-2, the upstream area, have high percolation rate while zones 3-4, the downstream area, have low percolation rate (see constant loss, f_c, in Table 1). Therefore, the excess rainfall intensities in the upstream part are generally lower than those in the downstream part. These excess rainfall intensities are shown in Table 7. For large rainfall, like 10-year rainfall, the excess rainfall intensity in the upstream part, zones 1-2, is not much lower than that in the downstream part, zones 3-4, regardless of whether it is a short duration, like 24-hour, or long duration, like 72-hour, rainfall. For small rainfall, like 2-year rainfall, the excess rainfall intensity in the downstream part is much lower than that in the upstream part for long duration rainfall, but still not much lower for short duration rainfall.

TABLE 7 PEAK EXCESS RAINFALL INTENSITIES IN ZONES 1-4

Return period (year)	Duration (hour)	Peak rainfall intensity (mm/h)	Peak excess rainfall intensity (mm/h)				
			Average	Zone 1	Zone 2	Zone 3	Zone 4
2	24	6.6	4.0	3.7	3.6	4.4	4.3
2	48	5.7	3.7	2.5	2.5	5.1	5.1
2	72	5.0	3.0	1.8	1.8	4.4	4.5
5	24	9.2	7.4	6.3	6.2	8.8	8.6
5	48	7.8	5.7	4.5	4.5	7.1	7.1
5	72	6.6	4.8	3.5	3.5	6.1	6.1
10	24	11.5	9.7	8.7	8.5	11.1	10.9
10	48	10.0	8.2	6.9	7.0	9.6	9.6
10	72	8.3	6.5	5.2	5.3	7.9	8.2

The large spatial difference among excess rainfall intensities for small rainfall with long duration can be described by the low rainfall intensity. With that low intensity, the influence of percolation is large, and due to the high percolation rate over the upstream area, the portion of the excess rainfall from that part is less. Therefore, the excess rainfall portion from the downstream part is dominant. On the other hand, when the rainfall magnitude is larger, the intensity increases, and therefore influence of percolation is less. Hence, more portion of the excess rainfall from the upstream part can occur. With this reason, the portion of excess rainfall from the upstream part increases with the rainfall intensity.

Since the middle and lower Yom basin is long and has non-uniform spatial characteristics, the lag time between rainfall and peak discharge varies upon rainfall location. Fig. 8 shows the hydrographs at the station Y4 from the 3-hour excess rainfall with the volume of 10 mm which occurs over the entire area of zones 1-4 and concentrates over each zone. It can be seen that from the most upstream zone, zone 1, to the station Y4, the lag time is approximately 72 hours, while from the others zone, zones 2-4, to the station Y4, the lag time is approximately 48 hours.

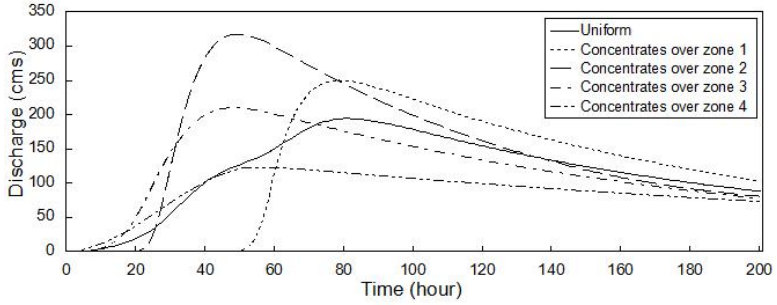

Fig. 8 Hydrograph at the station Y4 from 3-hour 10 mm excess rainfall which concentrates over each zone. Note that the rainfall volume is preserved and is equal to 10 mm multiplied by the size of the entire area of zones 1-4

DOI:10.5963/JWRHE0603001

As mentioned above, for the low intensity rainfall, most of the excess rainfall comes from the downstream part with short lag time, while for the high intensity rainfall, more excess rainfall from the upstream part with longer lag time can occur. It can be inferred that the low intensity rainfall has lower lag time than the high intensity rainfall. Since the lag time is related with the concentration time, it can be concluded that the small rainfall has shorter critical duration than the large rainfall.

IV. CONCLUSIONS

By removing the assumption of uniform basin characteristics in the middle and lower Yom basin, this study can simulate the variation of critical rainfall duration according to its magnitude. The larger rainfall appears to have longer critical duration as supported by the flood mitigation plan which suggests that the delay time of the predicted downstream water level after the observed upstream water level is longer for larger flood and shorter for smaller flood. Because the downstream part of the area is composed of clay as a major soil texture and has agricultural land as a major land cover while the upstream part is composed of coarser soil texture and has forest area as a major land cover, the percolation rate in the upstream part is higher than that in the downstream part. This difference of the percolation rates causes the variation of critical rainfall duration. When the rainfall intensity is low, a large portion of the rainfall over the upstream part becomes percolation loss, and as a result, most of the runoff tends to come from the downstream part which has shorter lag time. Oppositely, when the rainfall intensity is high, the influence of percolation becomes small, and as a result, more portion of runoff from the upstream part which has longer lag time can occur. Therefore, the larger rainfall has longer critical duration than the smaller rainfall.

Our finding points out that using the fixed critical rainfall duration may not be applicable for extreme flood mitigation when the basin characteristics is not uniform since the peak discharge under some specified return period can be underestimated. Not only in the middle and lower Yom basin, the flood mitigation plan also mentions the variability of the delay time of the expected water level at the downstream station after the observed water level at the upstream station in others area. Even though the delay time is not much variate for most of the area, it is found to be variate in some parts of the mountainous region in the northern and southern parts of Thailand. Also the direction of variation can be different. Mostly, the larger flood has shorter delay time. However, in some area such as our study area, larger flood has longer delay time. It is suggested that studying the variation of concentration time is useful for extreme flood simulations as it can help specifying the appropriate duration of the simulated rainfall for each return period, especially when the area is not uniform.

ACKNOWLEDGMENT

The financial support for this study has been provided by Japanese government scholarship and the Ratchadaphiseksomphot Endowment Fund 2016 of Chulalongkorn University (CU-59-057-CC). The data for this study has been supported by the Royal Irrigation Department and Thai Meteorological Department.

REFERENCES

[1] A. K. Fleig and D. Wilson, *NIFS - Flood Estimation in Small Catchments*, Norway: Norwegian Water Resources and Energy Directorate, 2013.

[2] U.S. Department of Agriculture, Natural Resources Conservation Service, *Chapter 15 Time of Concentration, National Engineering Handbook, Part 630 Hydrology*, U.S.: U.S. Department of Agriculture, Natural Resources Conservation Service, 2010.

[3] T. Tingsanchali and F. Karim, "Flood-hazard assessment and risk-based zoning of a tropical flood plain: Case study of the Yom River, Thailand", *Hydrological Sciences Journal*, vol. 55(2), pp. 145-161, 2010.

[4] Office of Water Management and Hydrology, Royal Irrigation Department, *Plan for Protection and Mitigation of Water-related Disasters (Rainy Season) in 2558 B.E.*, Thailand: Office of Water Management and Hydrology, Royal Irrigation Department, 2015. (in Thai)

[5] G. W. Brunner, *HEC-RAS, River Analysis System Hydraulic Reference Manual*, U.S.: Hydrologic Engineering Center, U.S. Army Corps of Engineers, 2010.

[6] A. D. Feldman, *Hydrologic Modeling System HEC-HMS: Technical Reference Manual*, U.S.: Hydrologic Engineering Center, U.S. Army Corps of Engineers, 2000.

[7] G. Lee, Y. Tachikawa, T. Sayama, and K. Takara, "Effect of spatial variability of rainfall on catchment responses in mesoscale mountainous area", *Annual Journal of Hydraulic Engineering*, vol. 53, pp. 7-12, 2009.

[8] S. Kotsuki and K. Tanaka, "Impacts of mid-rainy season rainfall on runoff into the Chao Phraya River, Thailand", *Journal of Disaster Research*, vol. 8(3), pp. 397-405, 2013.

[9] V. P. Singh, *Elementary Hydrology*, U.S.: Prentice Hall, 1992.

[10] E. S. Martins and J. R. Stedinger, "Generalized maximum-likelihood generalized extreme-value quantile estimators for hydrologic data", *Water Resources Research*, vol. 36(3), pp. 737-744, 2000.

DOI:10.5963/JWRHE0603001